Flight Mechanics Analysis of a Motorized Trike with Composite Wing

E. Carrera[1] and C. Cosatto[2]

Abstract: In this work, a mathematical model to study the dynamic behavior of a trike ultralight aircraft is developed. This is done because, to the best of the writers' knowledge, no specific theories are available for powered hang gliders. To do that, in order to take into account the engine thrust, the necessary changes have been made on models developed for hang gliders. The trike, which is a particular case of powered hang glider, is modeled as a compound system made of a wing and an undercarriage. The case of rigid wing, made of composite materials, is considered in the present work. Equilibrium governing equations are written, the trim conditions are evaluated, and the fixed control dynamic stability is investigated for both longitudinal and lateral motion. After that a modified wing configuration, with two additional vertical fins, is investigated and compared. The dynamic response to pilot controls is evaluated to complete the analysis.

DOI: 10.1061/(ASCE)AS.1943-5525.0000038

CE Database subject headings: Aircraft; Composite materials.

Author keywords: Ultralight aircraft.

Introduction

In recent years, many studies have been devoted to developing ultralight and light sport aircraft (LSA) with even more enhanced performance. These aircraft are characterized by low weight, low cost and some containments on the flight envelope and operative limitations. However, the low costs and the reduction in the certification bureaucracy make these vehicles more affordable than civil aviation so at the moment this is booming in the market. There are different types of ultralights or LSAs: fixed wing, trikes, powered parachutes, gyrocopters, and others. The fixed wing ones look like traditional light aircraft but have some weight and number of occupants' limitations. Trikes are hang gliders with a tricycle undercarriage and Powered Parachutes consisting of a parachute with an undercarriage. Gyrocopters look like helicopters but the rotor is not powered, its rotation is caused by the forward motion.

An ultralight or LSA trike consists of a hang glider wing and an undercarriage which is hanging under it. The wing is only bigger and stiffer to handle the increased weight. The undercarriage is equipped with seats for the occupants (one or two), an instrument panel, the landing gear, an engine with a propeller and a fuel tank. Trikes do not have flight controls like those used in fixed wing aircraft and they are controlled by shifting the pilot's weight side to side and fore and aft.

At the moment, trikes use wings like hang gliders, made of tubes and canvas. This means that the wing has the great advantage of being folded, but on the other hand, it needs boring tweak operations every time it is mounted on the undercarriage. In addition, this type of wing is flexible and can change its geometry and aerodynamic properties in function of the flight speed. However, a rigid wing may have some advantages compared to the traditional trike wings. For instance, the annoying tune operations can be avoided and the wing structure could be lighter than those that are made of tubes and canvas, and its aerodynamic properties remain the same for each flight condition. In addition, it is possible to improve the aerodynamic efficiency of the wing and reduce fuel consumption.

The particular configuration of wing plus hinged undercarriage makes trikes significantly different from conventional airplanes, even in flight dynamics. First of all, the pilot does not control it by deflecting mobile surfaces but with the method of weight shifting. This means that the pilot moves in order to change the position of the center of gravity (cg). This causes variations in the aerodynamic moments and modifies the flight path. Moreover hang gliders are tailless aircraft, so the longitudinal and lateral stability are provided only by the wing's own stability and the relative position of the center of gravity and wing's neutral point.

The absence of the tail implies that the pilot must trim the trike in the same way as the pilot controls it, so the relative distance between cg and neutral point changes for each trimmed flight condition and aircraft's stability properties varies at each flight speed. In addition, the engine is mounted on the undercarriage so the thrust's direction changes when the pilot changes position. These considerations make it clear that describing the flight dynamics of an ultralight trike is more difficult than describing that of a conventional airplane. As a consequence, the classical flight dynamics equations cannot be directly used.

To the best of the writers' knowledge, specific theories on flight dynamics of a powered hang glider are not available. A

[1]Professor of Aerospace Structures and Computational Aeroelasticity, Dept. of Aeronautics and Space Engineering, Politecnico di Torino, Corso Duca degli Abruzzi, 24, 10129 Torino, Italy (corresponding author). E-mail: erasmo.carrera@polito.it

[2]Research Assistant, Dept. of Aeronautics and Space Engineering, Politecnico di Torino, Corso Duca degli Abruzzi, 24, 10129 Torino, Italy. E-mail: cristian.cosatto@polito.it

Note. This manuscript was submitted on April 24, 2009; approved on December 28, 2009; published online on September 15, 2010. Discussion period open until March 1, 2011; separate discussions must be submitted for individual papers. This paper is part of the ***Journal of Aerospace Engineering***, Vol. 23, No. 4, October 1, 2010. ©ASCE, ISSN 0893-1321/2010/4-251–264/$25.00.

J. Aerosp. Eng. 2010.23:251-264.

model developed for hang gliders is modified in this work to consider the thrust's effects. Only a few works were published on flight dynamics of hang gliders, such as the studies made by De Matteis (1991), and Cook (1994) and Spottiswoode and Cook (2006). The kinematic formulations of these mathematical models are very similar in the case of fixed controls. In fact, the differences only concern the choice of the wing's reference point. However, these works used different approaches for the aerodynamic forces and moments definition: rigid and deformable wing are considered by De Matteis (1991) and by Cook (1994) and Spottiswoode and Cook (2006), respectively. The mathematical model that evaluates the effects of the wing deformations was made by analyzing the experimental data obtained by Kilkenny (1984). The effect of the velocity as a change in wing twist, the effect of the chamber variations and the effect of the luff lines was taken by Kilkenny (1986). So they actually used a different wing at each flight speed and incidence.

In this work the dynamic behavior of an innovative ultralight trike is analyzed. The "innovation" lies in the fact that the trike mounts a "rigid wing" which is made by composite materials, e.g., carbon fiber. This is a further contribution to the work started by Grande (2007) and Cannone (2006) in their MS thesis, in which the preliminary aerodynamic design and the structural analysis were made.

The word "rigid" is probably not very appropriate in this case since the carbon fiber is still deformable. The word rigid is used to emphasize that the wing is no longer made by tubes and canvas and the wing geometry, including wing sections is kept by the stiffness of the carbon fiber. Even if the composite wing is still deformable, no aeroelastic deformations have been taken into account. This is due to the low aspect ratio of the wing and the relatively low flight speed. The aeroelastic effects could be neglected.

The present work is focused on the analysis of longitudinal and lateral dynamic stability and the evaluation of control characteristics of the obtained rigid wing trike. Since the wing is rigid, it is possible to neglect the deformations caused by velocity so it is possible to use the usual aerodynamic model to determine forces and moments. These quantities are obtained with the vortex lattice method (VLM). Therefore the models spread out by De Matteis (1991) and by Spottiswoode and Cook (2006) were taken and modified in order to consider thrust's effects.

The choice of the aerodynamic center as reference system made by Spottiswoode and Cook (2006) allows to write down clearer expressions for the equilibrium. The wing aerodynamic center is located on its *cg*, so all the forces and moments are computed referring to this point.

The paper has been organized in the following way: first of all, the mathematical model developed for trike's dynamics is presented, and secondly it is modified to consider the effects of vertical fins. After that a numerical assessment is made and the obtained results are shown and discussed, then the conclusions are reported.

Mathematical Model

Reference System and Geometry

The trike is defined as an undercarriage suspended below a wing. The undercarriage structure is attached to the central section of the wing at the hang point. With this configuration the pilot may control the aircraft by pushing and pulling the control bar, which changes the relative distance between pilot and the wing, see Fig. 1.

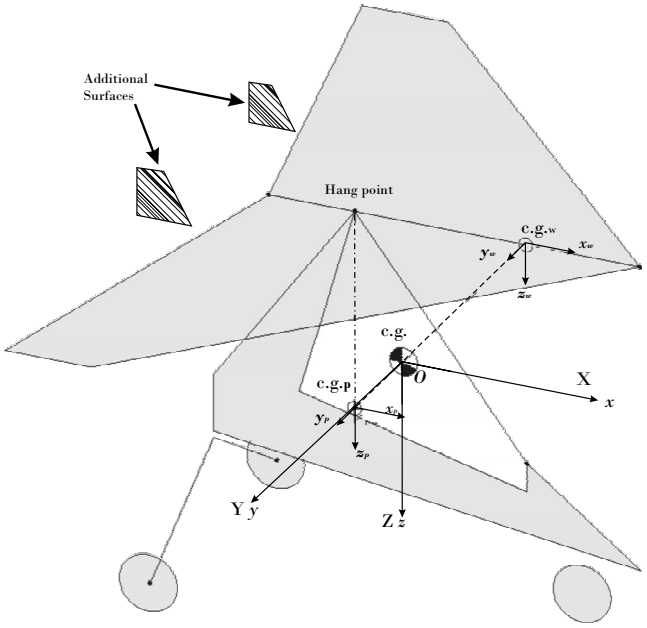

Fig. 1. Trike's outline and reference axes

As for the conventional aircraft, an orthogonal fixed body axis system (*oxyz*) is defined which origin coincides to the vehicle *cg*. The axes are arranged for trimmed conditions, the *x*-axis is parallel to the chord of the central section of the wing and the axes (*oxz*) define the plane of symmetry. The *cg* of the entire vehicle lies on the line that connects the *cg* of the wing and of the undercarriage. The location of wing's center of gravity, cg_w, is defined by the coordinates (x_w, y_w, z_w) while the center of gravity of the undercarriage, cg_p, is defined by coordinates (x_p, y_p, z_p). That is, the distance between cg_w and cg_p varies for each trim condition and the distance between the trike's *cg* and the aerodynamic center changes too. As a consequence, the aerodynamic and inertial moments about the system axes are different for each trim configuration. The trike is assumed to be rigid in its trim geometry, and small perturbations around trim state are considered. Furthermore, the mass matrix is constant for each trim state and the classical flight dynamics equations can be implemented.

Because of the considered geometry, the control variables will be the angles between the line that joins the hang point and the center of gravity of the undercarriage, and the line parallel to the *z*-axis at the hang point. The longitudinal control δ is the angle that lies in the longitudinal plane (*oxz*) and lateral control ξ is the angle which is lying in the plane (*oyz*). Positive directions are as shown in Fig. 2.

Equations of Motion

The equations of motion in Newtonian form are written in body axes reference as in Etkin (1995)

$$m(\dot{\mathbf{v}} + \tilde{\omega}\mathbf{v}) = \mathbf{F} = \mathbf{F_g} + \mathbf{F_a}$$

$$\dot{\mathbf{I}}\omega + \mathbf{I}\dot{\omega} + \tilde{\omega}\mathbf{I}\omega = \mathbf{M} = \mathbf{M_g} + \mathbf{M_a} \quad (1)$$

J. Aerosp. Eng. 2010.23:251-264.

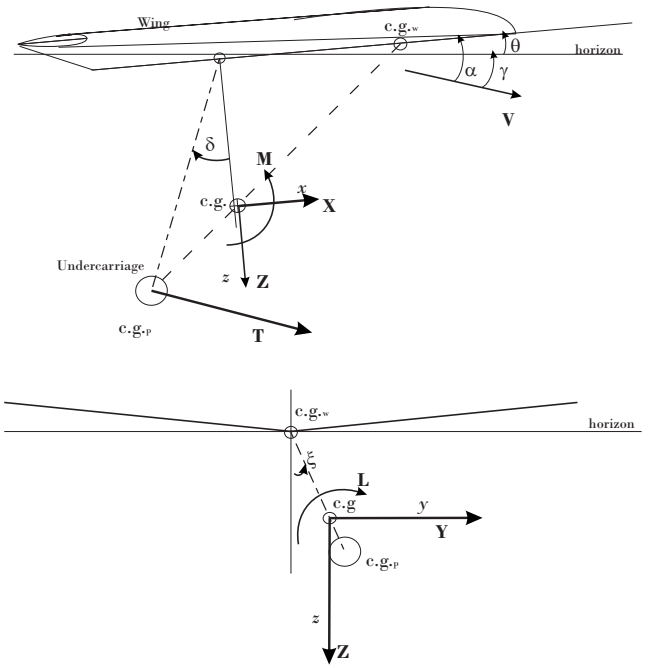

Fig. 2. Trike's geometry

where $\mathbf{F_g}$, $\mathbf{M_g}$=forces and moments due to gravity and $\mathbf{F_a}$, $\mathbf{M_a}$ =aerodynamic forces and moments. Thrust forces and moments are not explicitly shown in that notation, they are included into the aerodynamic terms, m and $\mathbf{I}$ are the whole mass and inertial matrix of the trike. As verified a posteriori the $\dot{\mathbf{I}}\boldsymbol{\omega}$ term could be considered negligible.

By considering symmetric trimmed flight and applying the principle of small perturbations, the following system of equations is obtained

$$m(\dot{u} + qw_{\text{eq}}) = X_a + X_g$$

$$m(\dot{v} - pw_{\text{eq}} + ru_{\text{eq}}) = Y_a + Y_g$$

$$m(\dot{w} - qu_{\text{eq}}) = Z_a + Z_g$$

$$I_x\dot{p} - I_{xz}\dot{r} = L_a + L_g$$

$$I_y\dot{q} = M_a + M_g$$

$$I_z\dot{r} - I_{xz}\dot{p} = N_a + N_g \tag{2}$$

where velocities, forces, and moments are defined as in Etkin (1995).

Forces and Moments due to Gravity

Since the origin of axes coincides with the center of gravity, only the wing and undercarriage weights survive, all the moments caused by these weights were canceled. By considering the small perturbation form, the following equations are obtained

$$X_g = -mg(\theta \cos \theta_{\text{eq}} + \sin \theta_{\text{eq}})$$

$$Y_g = mg\phi \cos \theta_{\text{eq}}$$

$$Z_g = mg(\cos \theta_{\text{eq}} - \theta \sin \theta_{\text{eq}})$$

$$L_g = M_g = N_g = 0 \tag{3}$$

where the whole mass of the trike is simply the sum of wing and undercarriage masses, $m=m_w+m_p$. The pilots, the engine and fuel masses are included in the undercarriage mass.

Aerodynamic Forces and Moments

Aerodynamic forces and moments referred to the center of gravity are given by the sum of wing and undercarriage contributions. But these contributions are defined with respect to their local centers of gravity and have to be referred by the vehicle cg. The local axes are parallel to the main ones and centered on their respective cg. By referring the local forces and moments to the trikes cg, aerodynamic forces are obtained

$$X_a = X_w + X_p$$

$$Y_a = Y_w + Y_p$$

$$Z_a = Z_w + Z_p$$

$$L_a = (L_w + y_wZ_w - z_wY_w) + (L_p + y_pZ_p - z_pY_p)$$

$$M_a = (M_w - x_wZ_w + z_wX_w) + (M_p - x_pZ_p + z_pX_p)$$

$$N_a = (N_w + x_wY_w - y_wX_w) + (N_p + x_pY_p - y_pX_p) \tag{4}$$

By considering small perturbations, forces and moments can be split in the stationary and perturbation parts, where the subscripts $(.)_{\text{eq}}$ indicates a stationary quantity and those without subscripts are the perturbations. In steady symmetric trimmed flight conditions, lateral force and moments are equal to zero so it is possible to write

$$Y_{w_{\text{eq}}} = L_{w_{\text{eq}}} = N_{w_{\text{eq}}} = 0$$

$$Y_{p_{\text{eq}}} = L_{p_{\text{eq}}} = N_{p_{\text{eq}}} = 0 \tag{5}$$

The engine's thrust is not explicitly indicated, but it is included in the aerodynamic forces of the undercarriage. The engine, in fact, is mounted just after the pilot seat. It was assumed that the thrust axis contains the cg of the undercarriage and it is normal to the line which joins the hang point and its cg.

It is also possible to write down wing and undercarriage positions in terms of small perturbations, where $y_{p_{\text{eq}}}=y_{w_{\text{eq}}}=0$ for symmetric flight conditions. The Eq. (4) then becomes a sum of equilibrium and perturbation components.

As it was assumed in De Matteis (1991) and Spottiswoode and Cook (2006), the only aerodynamic force which acts on the undercarriage is drag. In addition, it is assumed that the drag coefficient remains the same at each flight condition. This assump-

J. Aerosp. Eng. 2010.23:251-264.

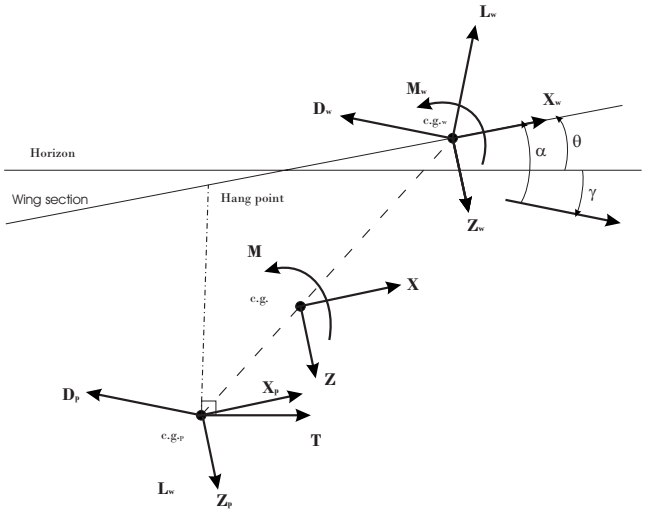

Fig. 3. Forces outline

tion was verified for the pilot by Kilkenny (1986) by a campaign of wind tunnel tests. And it is considered valid in the present work because the undercarriage is a nonlifting body too.

Forces acting on wing and undercarriage are depicted in Fig. 3. It is assumed that the thrust vector is normal to the line that joins the hang point and the *cg* of the undercarriage.

The aerodynamic forces are written in terms of derivatives to motion variables. For the wing is obtained

$$F_w = F_{u_w} u_w + F_{w_w} w_w + F_{q_w} q_w \tag{6}$$

where, according to Spottiswoode and Cook (2006), the $\dot{w}$ terms are considered negligible. The perturbations in the velocities (written in terms of the vehicle *cg*) values are

$$u_w = u + qz_w - ry_w = u + qz_w \quad p_w = p$$

$$v_w = v - px_w + rx_w \quad q_w = q$$

$$w_w = w - qx_w + py_w = w - qx_w \quad r_w = r \tag{7}$$

Upon substitution of Eq. (7) in Eq. (6), the perturbations of the wing can be described in terms of the whole aircraft velocities

$$X_w = X_{u_w} u + X_{w_w} w + (-x_{w_{eq}} X_{w_w} + z_{w_{eq}} X_{u_w}) q$$

$$Y_w = Y_{v_w} v - z_{w_{eq}} Y_{v_w} p + x_{w_{eq}} Y_{v_w} r$$

$$Z_w = Z_{u_w} u + Z_{w_w} w + (Z_{q_w} + z_{w_{eq}} Z_{u_w} - x_{w_{eq}} Z_{w_w}) q$$

$$L_w = L_{v_w} v + (L_{p_w} - z_{w_{eq}} L_{v_w}) p + (L_{r_w} + x_{w_{eq}} L_{v_w}) r$$

$$M_w = M_{u_w} u + M_{w_w} w + (M_{q_w} - x_{w_{eq}} M_{w_w} + z_{w_{eq}} M_{u_w}) q$$

$$N_w = N_{v_w} v + (N_{p_w} - z_{w_{eq}} N_{v_w}) p + (N_{r_w} + x_{w_{eq}} N_{v_w}) r \tag{8}$$

where it has been assumed that $X_{q_w} = Y_{p_w} = Y_{r_w} \simeq 0$.

Then in the same way for the undercarriage is obtained

$$X_p = X_{u_p} u + X_{w_p} w + (-x_{p_{eq}} X_{w_p} + z_{p_{eq}} X_{u_p}) q \quad L_p = 0$$

$$Y_p = Y_{v_p} v - z_{p_{eq}} Y_{v_p} p + x_{p_{eq}} Y_{v_p} r \quad M_p = M_{q_p} q$$

$$Z_p = Z_{u_p} u + Z_{w_p} w + (z_{p_{eq}} Z_{u_p} - x_{p_{eq}} Z_{w_p}) q \quad N_p = N_{r_p} r \tag{9}$$

the assumption permits us to introduce the following simplification:

$$\begin{matrix} & M_{u_p} = M_{w_p} = 0 & \\ X_{q_p} = Z_{q_p} = 0 & & \\ Y_{p_p} = Y_{r_p} = 0 & L_{v_p} = L_{p_p} = L_{r_p} = 0 & \\ & & \\ & N_{v_p} = N_{p_p} = 0 & \end{matrix} \tag{10}$$

It is convenient to write the undercarriage and wing positions (x, y, z) in terms of the control angles (δ, ξ). As a consequence, the number of control variables is reduced from six to two. As seen in Fig. 4, these quantities are also proportional to mass ratios, as in Eq. (11) and Eq. (12). For the longitudinal control one has

$$x_w = \frac{m_p}{m}(l_1 + l_2 \sin\delta) \quad z_w = -\frac{m_p}{m} l_2 \cos\delta$$

$$x_p = -\frac{m_w}{m}(l_1 + l_2 \sin\delta) \quad z_p = \frac{m_w}{m} l_2 \cos\delta \tag{11}$$

while for lateral control

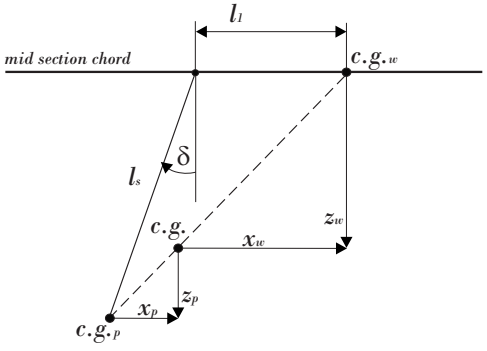

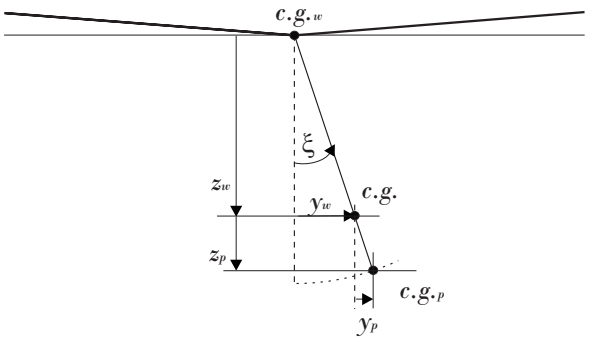

Fig. 4. Longitudinal and lateral control geometry

J. Aerosp. Eng. 2010.23:251-264.

$$y_w = -\frac{m_p}{m} l_2 \cos\delta \sin\xi; \quad z_w = -\frac{m_p}{m} l_2 \cos\delta \cos\xi$$

$$y_p = \frac{m_w}{m} l_2 \cos\delta \sin\xi; \quad z_p = \frac{m_w}{m} l_2 \cos\delta \cos\xi \tag{12}$$

Splitting the control angles into equilibrium term and perturbation and by considering symmetric trim flight conditions, $y_{w_{eq}} = y_{p_{eq}} = \xi_{eq} = 0$, it is possible to write the wing and undercarriage positions as in the following:

$$x_{w_{eq}} + x_w = k_p((l_1 + l_2 \sin\delta_e) + (l_2 \cos\delta_{eq})\delta)$$

$$y_{w_{eq}} + y_w = 0 + k_p(-l_2 \cos\delta_{eq})\xi$$

$$z_{w_{eq}} + z_w = k_p(-l_2 \cos\delta_{eq} + (l_2 \sin\delta_{eq})\delta)$$

$$x_{p_{eq}} + x_p = k_w(-(l_1 + l_2 \sin\delta_e) - (l_2 \cos\delta_{eq})\delta)$$

$$y_{p_{eq}} + y_p = 0 + k_w(l_2 \cos\delta_{eq})\xi$$

$$z_{p_{eq}} + z_p = k_w(l_2 \cos\delta_{eq} - (l_2 \sin\delta_{eq})\delta) \tag{13}$$

where $k_p = (m_p/m) e k_w = (m_w/m)$.

By collecting all the terms referred to each variable, it is possible to write the aerodynamic forces in a compact notation introducing the equivalent derivatives that are to be terms with star $(.)^*$

$$X_a = X_{a_{eq}} + X_u^* u + X_w^* w + X_q^* q + X_{\delta_{th}}^* \delta_{th}$$

$$Y_a = Y_v^* v + Y_p^* p + Y_r^* r$$

$$Z_a = Z_{a_{eq}} + Z_u^* u + Z_w^* w + Z_q^* q + Z_{\delta_{th}}^* \delta_{th}$$

$$L_a = L_v^* v + L_p^* p + L_r^* r + L_\xi^* \xi + L_{\delta_{th}}^* \delta_{th}$$

$$M_a = M_{a_{eq}} + M_u^* u + M_w^* w + M_q^* q + M_\delta^* \delta + M_{\delta_{th}}^* \delta_{th}$$

$$N_a = N_v^* v + N_p^* p + N_r^* r + N_\xi^* \xi + N_{\delta_{th}}^* \delta_{th} \tag{14}$$

These derivatives are the same as in Spottiswoode and Cook (2006), and for the control variables these equivalent derivatives are

$$M_\delta^* = l_2[(k_w Z_{p_{eq}} - k_p Z_{w_{eq}})\cos\delta_{eq} + (k_w X_{p_{eq}} - k_p X_{w_e} \sin\delta_{eq})]$$

$$L_\xi^* = l_2(k_w Z_{p_{eq}} - k_p Z_{w_{eq}})\cos\delta_{eq}$$

$$N_\xi^* = l_2(-k_w X_{p_{eq}} + k_p X_{w_{eq}})\cos\delta_{eq}$$

$$X_{\delta_{th}}^* = X_{\delta_{th_p}}$$

$$Z_{\delta_{th}}^* = Z_{\delta_{th_p}}$$

$$M_{\delta_{th}}^* = -z_{p_{eq}} X_{\delta_{th}}^* - x_{p_{eq}} Z_{\delta_{th}}^* \tag{15}$$

Linearized Equations of Motion

Substituting Eqs. (3) and (14) into Eq. (2), it is possible to obtain the linearized equations of motion

$$m\dot{u} = X_{a_{eq}} + X_u^* u + X_w^* w + (X_q^* - m w_{eq}) q - mg(\theta \cos\theta_{eq} + \sin\theta_{eq})$$

$$m\dot{v} = Y_v^* v + (Y_p^* + m w_{eq}) p + (Y_r^* - m u_{eq}) r + mg\phi \cos\theta_{eq}$$

$$m\dot{w} = Z_{a_{eq}} + Z_u^* u + Z_w^* w + (Z_q^* + m u_{eq}) q + mg(\cos\theta_{eq} - \theta \sin\theta_{eq})$$

$$I_x \dot{p} - I_{xz} \dot{r} = L_v^* v + L_p^* p + L_r^* r + L_\xi^* \xi$$

$$I_y \dot{q} = M_{a_{eq}} + M_u^* u + M_w^* w + M_q^* q + M_\delta^* \delta$$

$$I_z \dot{r} - I_{xz} \dot{p} = N_v^* v + N_p^* p + N_r^* r + N_\xi^* \xi \tag{16}$$

The terms of the equations which are related to the symmetric trimmed flight conditions can be deleted because their sum is equal to zero. Due to the linearization of motion, it is possible to decouple the longitudinal and lateral motions. The equations in state-space matrix formulation for the longitudinal motion are

$$\begin{bmatrix} m & 0 & 0 & 0 \\ 0 & m & 0 & 0 \\ 0 & 0 & I_y & 0 \\ 0 & 0 & 0 & 1 \end{bmatrix} \begin{Bmatrix} \dot{u} \\ \dot{w} \\ \dot{q} \\ \dot{\theta} \end{Bmatrix} = \begin{bmatrix} X_u^* & X_w^* & (X_q^* - m w_{eq}) & -mg\cos\theta_{eq} \\ Z_u^* & Z_w^* & (Z_q^* + m u_{eq}) & -mg\sin\theta_{eq} \\ M_u^* & M_w^* & M_q^* & 0 \\ 0 & 0 & 1 & 0 \end{bmatrix} \times \begin{Bmatrix} u \\ w \\ q \\ \theta \end{Bmatrix} + \begin{bmatrix} 0 & X_{\delta_{th}}^* \\ 0 & Z_{\delta_{th}}^* \\ M_\delta^* & M_{\delta_{th}}^* \\ 0 & 0 \end{bmatrix} \begin{Bmatrix} \delta \\ \delta_{th} \end{Bmatrix} \tag{17}$$

while for the lateral motion are as

$$\begin{bmatrix} m & 0 & 0 & 0 & 0 \\ 0 & I_x & -I_{xz} & 0 & 0 \\ 0 & -I_{xz} & I_z & 0 & 0 \\ 0 & 0 & 0 & 1 & 0 \\ 0 & 0 & 0 & 0 & 1 \end{bmatrix} \begin{Bmatrix} \dot{v} \\ \dot{p} \\ \dot{r} \\ \dot{\phi} \\ \dot{\psi} \end{Bmatrix} = \begin{bmatrix} Y_v^* & (Y_p^* + m w_{eq}) & (Y_r^* - m u_{eq}) & mg\cos\theta_{eq} & mg\sin\theta_{eq} \\ L_v^* & L_p^* & L_r^* & 0 & 0 \\ N_v^* & N_p^* & N_r^* & 0 & 0 \\ 0 & 1 & 0 & 0 & 0 \\ 0 & 0 & 1 & 0 & 0 \end{bmatrix} \times \begin{Bmatrix} v \\ p \\ r \\ \phi \\ \psi \end{Bmatrix} + \begin{bmatrix} 0 \\ L_\xi^* \\ N_\xi^* \\ 0 \\ 0 \end{bmatrix} \xi \tag{18}$$

J. Aerosp. Eng. 2010.23:251-264.

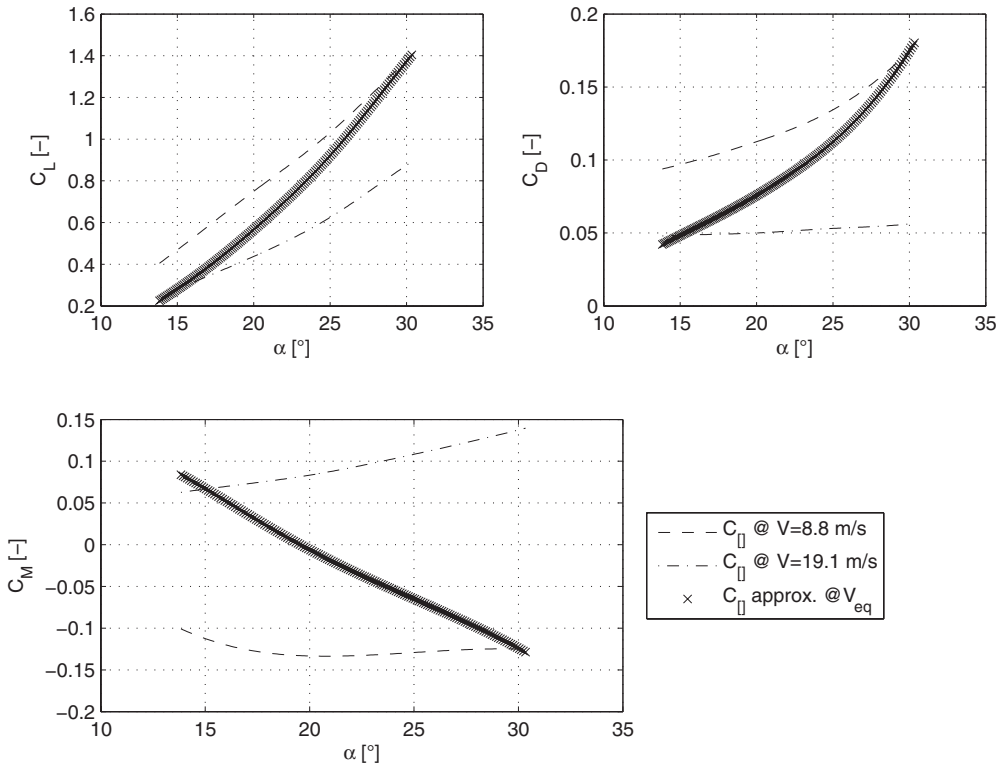

Fig. 5. Wing aerodynamics coefficients used in the numerical assessment

Derivative of Aerodynamic Forces

To evaluate the global forces and moments acting on the wing and for the evaluation of their aerodynamic derivatives, the VLM is used. To do that the software AVL, developed by Drela and Youngren (2008) is used.

It is assumed that the undercarriage produces only drag and that its lift and side force could be neglected. However the y and z components of the drag are included in the evaluation of its aerodynamic derivatives. The drag force produced by the undercarriage is mostly viscous drag that it is not possible to evaluate with VLM and requires a more complex calculation that is outside the purpose of the work. To perform the numerical assessment, the drag coefficients found in references were used.

Wing Aerodynamics

Because lift and drag are defined as normal and parallel to the velocity vector respectively, the forces X_w and Y_w are defined in wing body axes; and as for conventional aircraft, it is possible to use the Bryan's linear air reactions by Etkin (1995) where, according to Spottiswoode and Cook (2006), the $\dot{\alpha}$ and $\dot{q}$ terms are assumed negligible being the trike a tailless aircraft. To evaluate the dimensional derivatives the procedure by Etkin (1995) is used. For a detailed derivation of these quantities see Carrera and Cosatto (2008).

Undercarriage Aerodynamics

As mentioned above, the undercarriage produces only drag, but if a lateral or vertical component of velocity arises, the drag direction changes and a y or z component of force will be created

$$X_p = T\cos\delta - D_{p\text{eq}}\cos\alpha$$

$$Y_p = -(T\cos\delta - D_{p\text{eq}}\cos\alpha)\sin\beta$$

$$Z_p = T\sin\delta - D_{p\text{eq}}\sin\alpha \tag{19}$$

In addition the drag coefficient is assumed to be constant

$$D_{p_{\text{eq}}} = 1/2\rho V^2 S C_{D_{p\text{eq}}}$$

$$T = \frac{1}{2}\rho V^2 S C_{T_{\text{eq}}} + \frac{1}{2}\rho\frac{V^2}{u_{\text{eq}}} S C_{T_u} u + \frac{1}{2}\rho S V^2 C_{T_{\delta_{\text{th}}}}\delta_{\text{th}} \tag{20}$$

where the velocity is written in terms of small perturbations as

$$V^2 = (u_{\text{eq}} + u)^2 + v^2 + (w_{\text{eq}} + w)^2$$

To express the dimensional aerodynamic derivatives of the undercarriage, by referring to cg_p, one has

- Longitudinal derivatives

$$X_{u_p} = \frac{1}{2}\rho S\frac{w_{\text{eq}}^2}{u_{\text{eq}}}\cos\delta_{\text{eq}} C_{T_u} + \frac{1}{2}\rho S u_{\text{eq}}[-2C_{D_{p_{eq}}}\cos\alpha_{\text{eq}} + (2C_{T_{\text{eq}}} + C_{T_u})\cos\delta_{\text{eq}}]$$

$$Z_{u_p} = \frac{1}{2}\rho S\frac{w_{\text{eq}}^2}{u_{\text{eq}}} C_{T_u}\sin\delta_{\text{eq}} + \frac{1}{2}\rho S u_{\text{eq}}[-2C_{D_{p_{\text{eq}}}}\sin\alpha_{\text{eq}} + (2C_{T_{\text{eq}}} + C_{T_u})\sin\delta_{\text{eq}}]$$

$$M_{u_p} = 0$$

J. Aerosp. Eng. 2010.23:251-264.

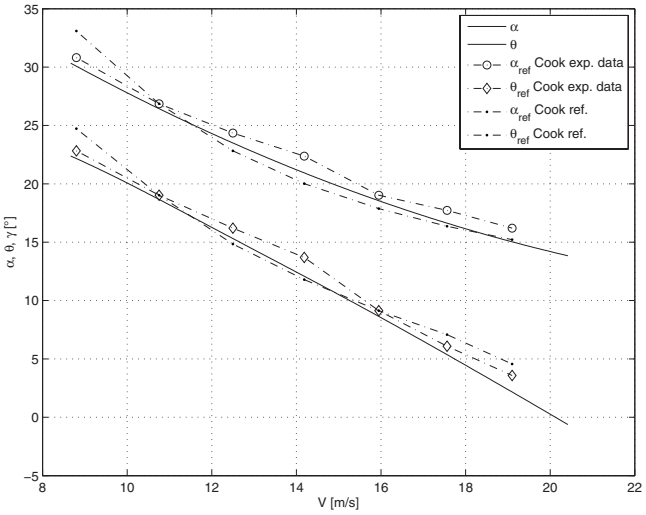

Fig. 6. α and θ angles in trimmed flight, comparison with reference

$$X_{w_p} = \frac{1}{2}S\rho w_{\text{eq}}(-2C_{D_{p_{\text{eq}}}}\cos\alpha_{\text{eq}} + 2C_{T_{\text{eq}}}\cos\delta_{\text{eq}}) + \frac{1}{2}\rho S\left(u_{\text{eq}} + \frac{w_{\text{eq}}^2}{u_{\text{eq}}}\right)C_{D_{p_{\text{eq}}}}\sin\alpha_{\text{eq}}$$

$$Z_{w_p} = -\frac{1}{2}\rho S\left(u_{\text{eq}} + \frac{w_{\text{eq}}^2}{u_{\text{eq}}}\right)C_{D_{p_{\text{eq}}}}\cos\alpha_{\text{eq}} + \frac{1}{2}\rho S w_{\text{eq}}(-2C_{D_{p_{\text{eq}}}}\sin\alpha_{\text{eq}} + 2C_{T_{\text{eq}}}\sin\delta_{\text{eq}})$$

$$M_{w_p} = 0$$

$$X_{q_p} = 0$$

$$Z_{q_p} = 0$$

$$M_{q_p} = 0 \tag{21}$$

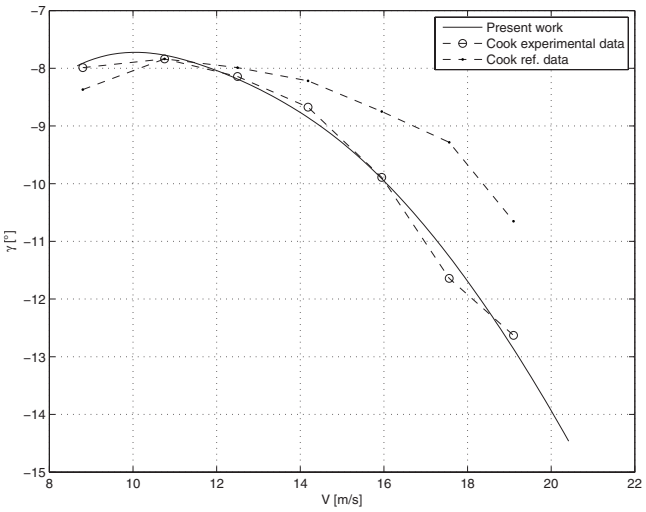

Fig. 7. Descent angle γ in trimmed conditions, comparison with reference

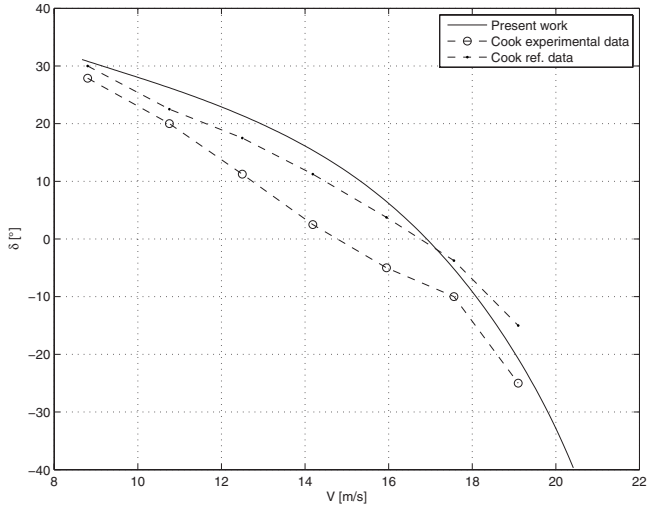

Fig. 8. Control angle δ in trimmed flight condition, comparison with reference

- Lateral derivatives; and

$$Y_{v_p} = \frac{1}{2}\rho S\left(u_{\text{eq}} + \frac{w_{\text{eq}}^2}{u_{\text{eq}}}\right)(-C_{D_{p_{\text{eq}}}}\cos\alpha_{\text{eq}} - C_{T_{\text{eq}}}\cos\delta_{\text{eq}})$$

$$L_{v_p} = 0$$

$$N_{v_p} = 0$$

$$Y_{p_p} = 0 \quad Y_{r_p} = 0$$

$$L_{p_p} = 0 \quad L_{r_p} = 0$$

$$N_{p_p} = 0 \quad N_{r_p} = 0 \tag{22}$$

- Thrust control derivatives

$$X_{\delta_{\text{th}_p}} = \frac{1}{2}\rho S C_{T_{\delta_{\text{th}}}}\cos\delta_{\text{eq}} \quad L_{\delta_{\text{th}_p}} = 0$$

$$Y_{\delta_{\text{th}_p}} = 0 \quad M_{\delta_{\text{th}_p}} = 0$$

$$Z_{\delta_{\text{th}_p}} = \frac{1}{2}\rho S C_{T_{\delta_{\text{th}}}}\sin\delta_{\text{eq}} \quad N_{\delta_{\text{th}_p}} = 0 \tag{23}$$

Table 1. Mass Properties of the Trike

Parameter	Units	Value (kg)
Wing mass	m_w	31
Pilot mass	m_{pil}	80
Undercarriage mass	$m_{\text{carr-mot}}$	100
Fuel mass	m_{carb}	80
Trike total mass (two pilots)	m_p	340

J. Aerosp. Eng. 2010.23:251-264.

Table 2. Aerodynamics and Geometric Characteristics of the Wing

Parameter	Symbol	Value
Wing area	S	16.26 m^2
Wing span	b	10 m
Reference chord	$c_{ref}=c_{m.g.}$	1.626 m
Distance between c_{ref} and wing nose	$x_{c_{ref}}$	1.26 m
Dihedral angle	Γ	1°
Twist angle	ϵ	−11°
Sweep angle	$\Lambda_{1/4c}$	24°
Aerodynamic reference point position	ξ_{arp}	21.5 % c_{ref}
Hang point position	ξ_{hang}	24.6 % c_{ref}
Distance between hang point and carriage cg	l_s	1.2 m
Undercarriage pilot drag coefficient	C_{D_p}	0.009

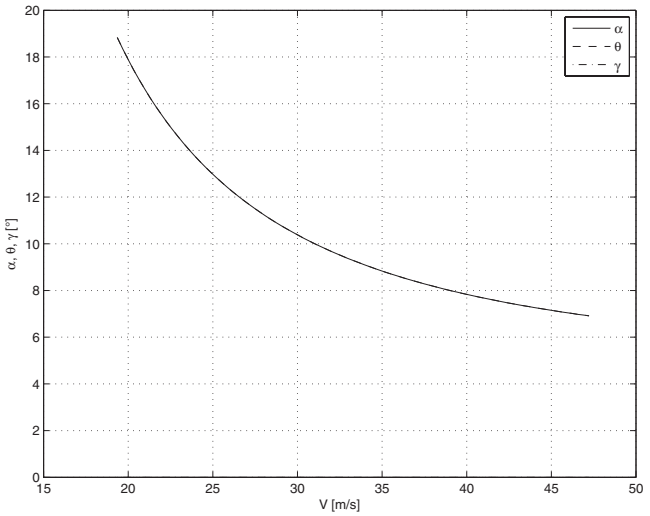

Fig. 9. α, γ, and θ angles in trimmed flight conditions

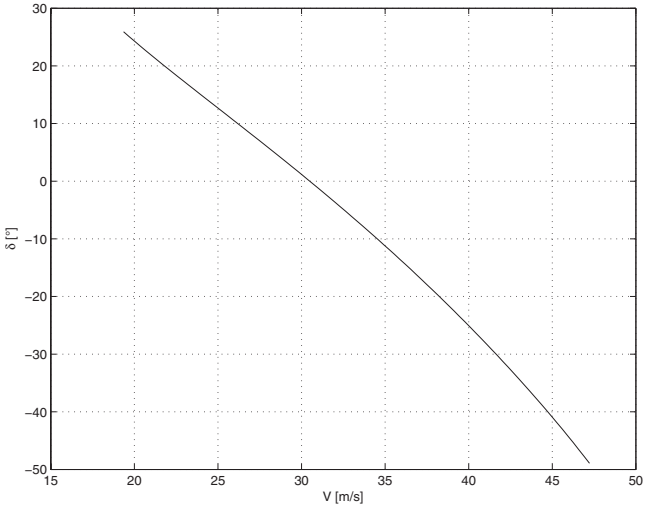

Fig. 10. Control angle δ in trimmed flight conditions

Modified Wing Configuration with Vertical Surfaces

As suggested by Cannone (2006), to improve lateral stability and control performances, two vertical surfaces were added to the wing, as seen in Fig. 1. The two fins have also mobile surfaces that could be deflected in the same or opposite direction, so it is possible to maneuver in both longitudinal and lateral motion. Each additional fin is positioned 3 m rearward from the wing nose and 2 m out of the plane of symmetry with a surface of 0.2 m^2 each. The fins are inclined outward with respect to the longitudinal plane of 15°, so little vertical forces could be generated.

To consider the control surfaces in the mathematical model, additional control terms related to the vertical surfaces must be added into the systems of equations [Eqs. (17) and (18)]. Adding these new terms, linear equations become as written in Eq. (24) for longitudinal motion and Eq. (25) for the lateral one

$$[\mathbf{M}_{long}]\begin{Bmatrix}\dot{u}\\ \dot{w}\\ \dot{q}\\ \dot{\theta}\end{Bmatrix}=[\mathbf{A}_{long}]\begin{Bmatrix}u\\ w\\ q\\ \theta\end{Bmatrix}+\begin{bmatrix}0 & X^*_{\delta_{t_{symm}}} & X^*_{\delta_{t_{symm}}} & X^*_{\delta_{th}}\\ 0 & Z^*_{\delta_{t_{symm}}} & Z^*_{\delta_{t_{asymm}}} & Z^*_{\delta_{th}}\\ M^*_{\delta} & M^*_{\delta_{t_{symm}}} & M^*_{\delta_{t_{asymm}}} & M^*_{\delta_{th}}\\ 0 & 0 & 0 & 0\end{bmatrix}\times\begin{Bmatrix}\delta\\ \delta_{t_{symm}}\\ \delta_{t_{asymm}}\\ \delta_{th}\end{Bmatrix} \tag{24}$$

$$[\mathbf{M}_{lat}]\begin{Bmatrix}\dot{v}\\ \dot{p}\\ \dot{r}\\ \dot{\phi}\\ \dot{\psi}\end{Bmatrix}=[\mathbf{A}_{lat}]\begin{Bmatrix}v\\ p\\ r\\ \phi\\ \psi\end{Bmatrix}+\begin{bmatrix}0 & Y^*_{\delta_{t_{symm}}} & Y^*_{\delta_{t_{asymm}}}\\ L^*_{\xi} & L^*_{\delta_{t_{symm}}} & L^*_{\delta_{t_{asymm}}}\\ N^*_{\xi} & N^*_{\delta_{t_{symm}}} & N^*_{\delta_{t_{asymm}}}\\ 0 & 0 & 0\\ 0 & 0 & 0\end{bmatrix}\begin{Bmatrix}\xi\\ \delta_{t_{symm}}\\ \delta_{t_{asymm}}\end{Bmatrix} \tag{25}$$

where new terms are defined as

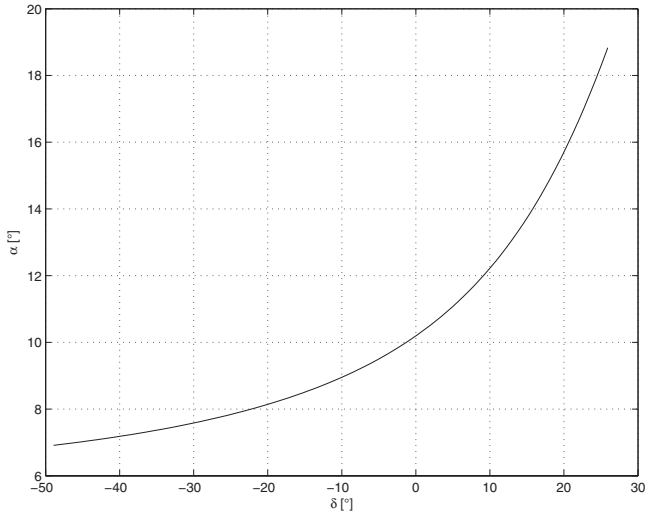

Fig. 11. Control angle δ versus incidence α, trimmed flight conditions

J. Aerosp. Eng. 2010.23:251-264.

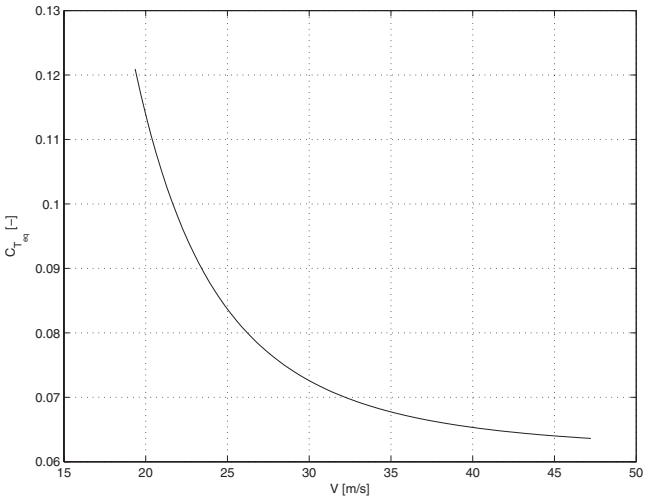

Fig. 12. Thrust coefficient in trimmed flight conditions

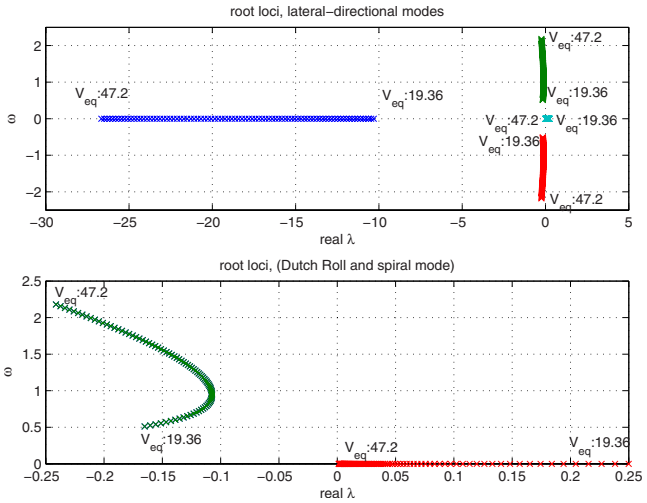

Fig. 14. Root loci for lateral-directional motion, dependence with the speed

$$X^*_{\delta_t} = X_{\delta_t} = \frac{1}{2}\rho S u_0^2 (C_{L_{\delta_t}} \sin\alpha_{eq} - C_{D_{\delta_t}} \cos\alpha_{eq})$$

$$Z^*_{\delta_t} = Z_{\delta_t} = \frac{1}{2}\rho S u_0^2 (-C_{L_{\delta_t}} \cos\alpha_{eq} - C_{D_{\delta_t}} \sin\alpha_{eq})$$

$$Y^*_{\delta_t} = Y_{\delta_t} = \frac{1}{2}\rho S u_0^2 C_{Y_{\delta_t}}$$

$$M^*_{\delta_t} = \frac{1}{2}\rho c_{ref} S u_0^2 C_{m_{\delta_t}} + l_s k_p X_{\delta_t} \cos\delta_{eq} - k_p (l_1 + l_s \sin\delta_{eq}) Z_{\delta_t}$$

$$L^*_{\delta_t} = \frac{1}{2}\rho b S u_0^2 C_{l_{\delta_t}} + l_s k_p Y_{\delta_t} \cos\delta_{eq}$$

$$N^*_{\delta_t} = \frac{1}{2}\rho b S u_0^2 C_{n_{\delta_t}} + k_p (l_1 + l_s \sin\delta_{eq}) Y_{\delta_t} \tag{26}$$

Control aerodynamic derivatives are computed using the VLM, as it was done for the wing.

Results and Discussion

Numerical Assessment

If the trike mounts the same wing used by Spottiswoode and Cook (2006), the engine is off and the whole weight of the undercarriage is the same as the weight of pilot considered in De Matteis (1991), the same results has to be obtained. Unfortunately

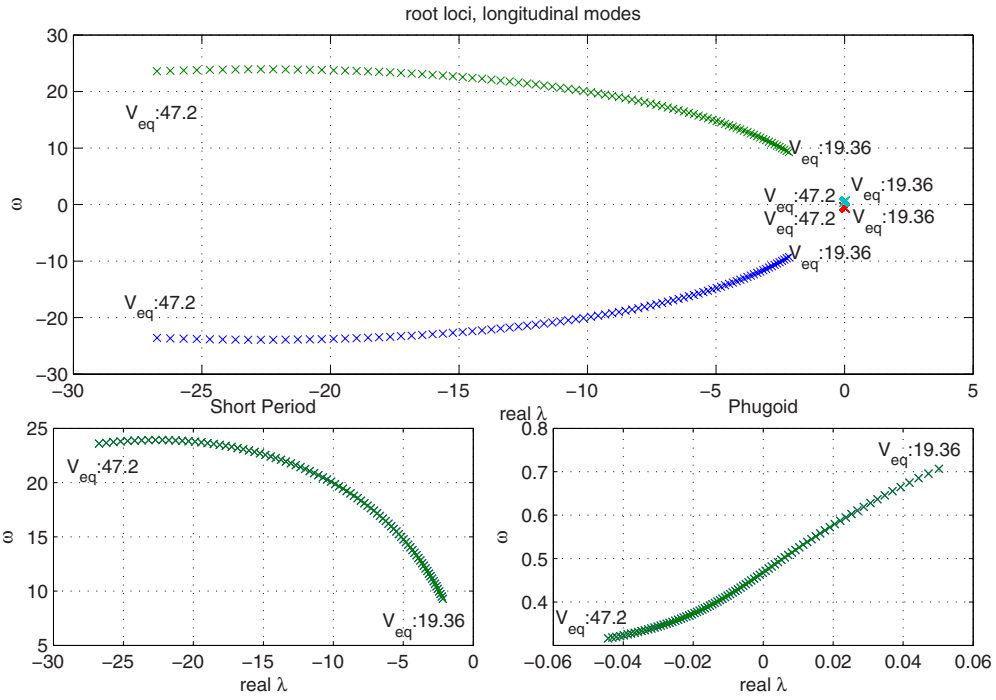

Fig. 13. Root loci for longitudinal motion, dependence with the speed

J. Aerosp. Eng. 2010.23:251-264.

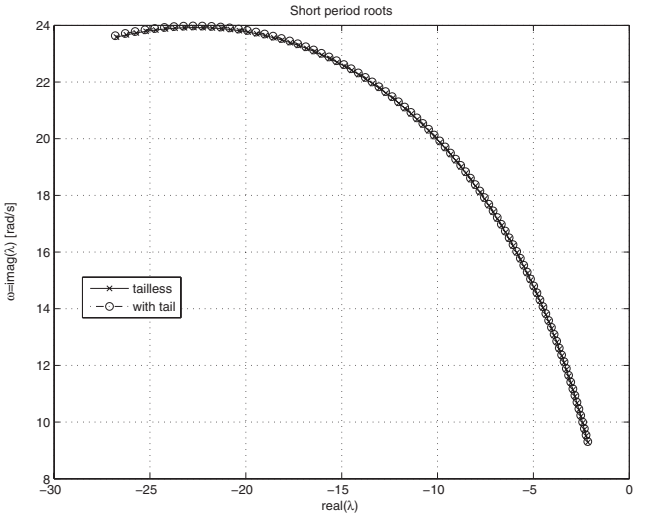

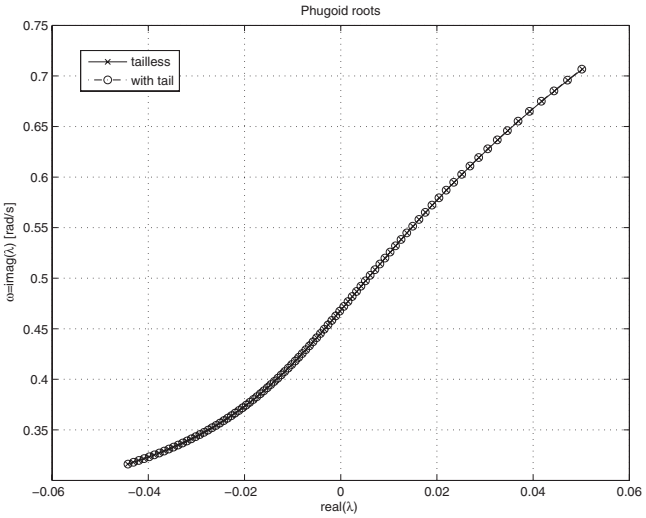

Fig. 15. Effects of vertical surfaces on longitudinal modes

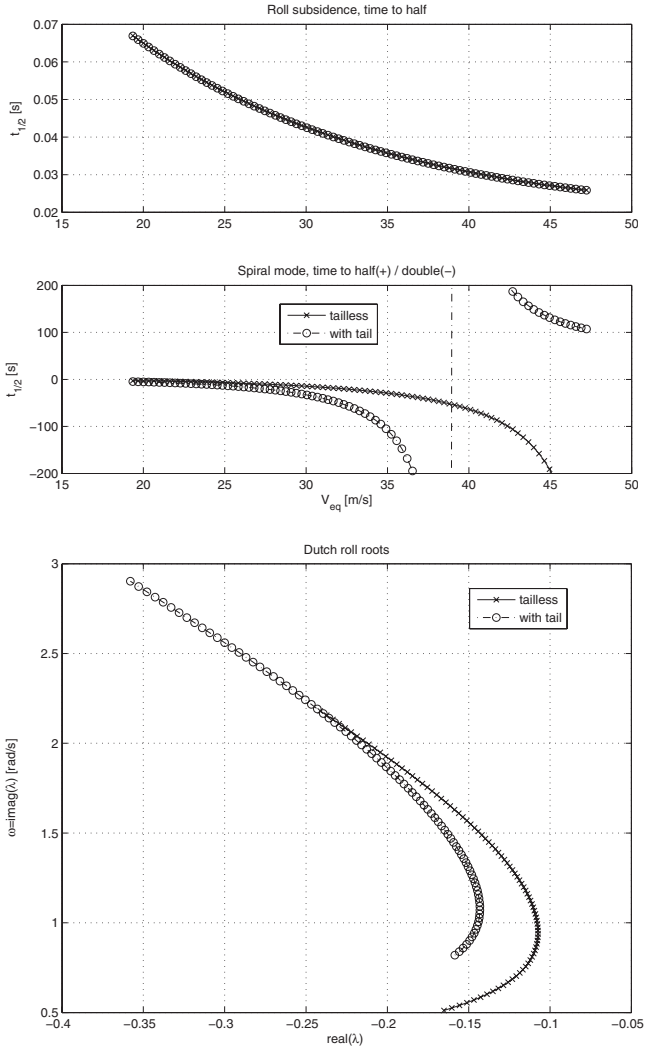

Fig. 16. Effects of vertical surfaces on lateral modes

a direct comparison cannot be made, because in Spottiswoode and Cook (2006) the aerodynamic characteristics of wing are not given. However, in De Matteis (1991) lift, drag, and pitching moment curves for two flight speeds are reported, so it was decided to use these values and evaluate the aerodynamic coefficients for the other velocities by interpolation. In Fig. 5 it is possible to see the aerodynamic coefficients used for this comparison.

Trim Conditions

As seen in Fig. 6–8, the results obtained for the trim conditions agree with both experimental data and Cook mathematical model. The main differences are found for the pilot control δ_{eq}. These are caused by the approximations in the evaluation of the aerodynamic coefficients.

To evaluate these quantities the procedure explained by Cook (1994) is used, apart from the control angle δ which is computed by solving numerically the momentum equilibrium to y-body axis.

Dynamic Stability

The aerodynamic derivatives are not reported by De Matteis (1991), so it was impossible make a concrete comparison with referenced dynamic stability results.

Results for Trike with Composite Wing

In case of powered flight it is better to impose, as trimmed conditions, that the flight is symmetric, at constant speed and at constant altitude. So the descent angle γ has to be imposed equal to zero. With this additional condition the other flight variables are defined at each fixed flight speed.

Mass properties are shown in Table 1, and the wing geometry properties in Table 2.

Trim Conditions

To evaluate the flight parameters for trimmed conditions, the equilibrium of stationary forces and moments were solved by taking into account the thrust and the different mass parameters of the aircraft. The results are reported in Fig. 9–12.

In Fig. 11 it is possible to see that by increasing the incidence of the wing the control angle δ must increase. This agrees with usual way of piloting this kind of aircraft. In addition, by looking at Fig. 10 it is possible to see that minimum and maximum speeds are not limited by the engine power or by the aerodynamic properties of the wing, such as lift or drag coefficients, but by the control geometry. This means that both the minimum and maximum speeds, in rectilinear steady horizontal flight, are limited by forces at pilot's control bar and its maximum displacements. For example, if the maximum speed is exceeded the trike will

J. Aerosp. Eng. 2010.23:251-264.

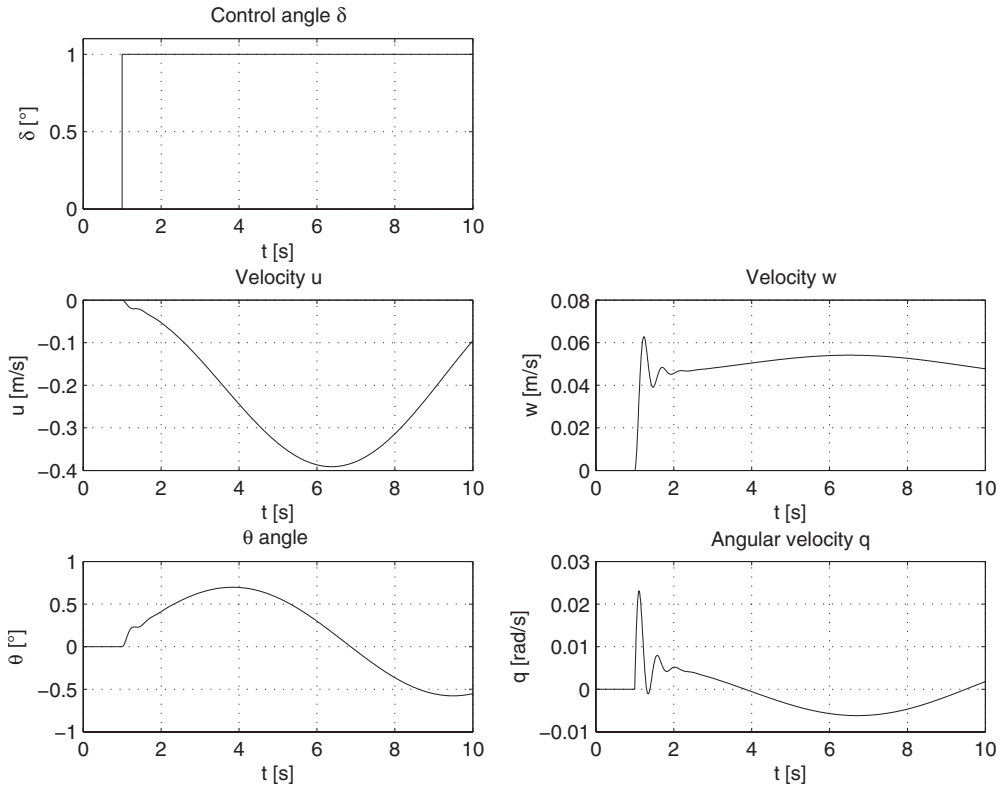

Fig. 17. Longitudinal response to a step δ_c=+1°

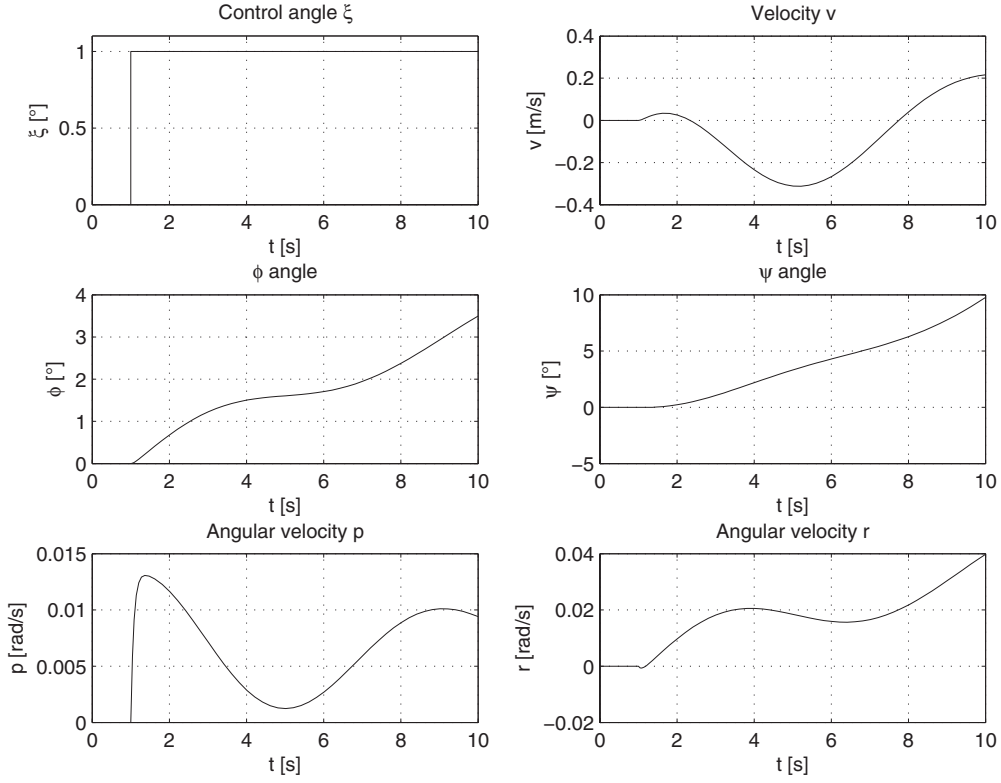

Fig. 18. Lateral response to a step ξ_c=+1°

J. Aerosp. Eng. 2010.23:251-264.

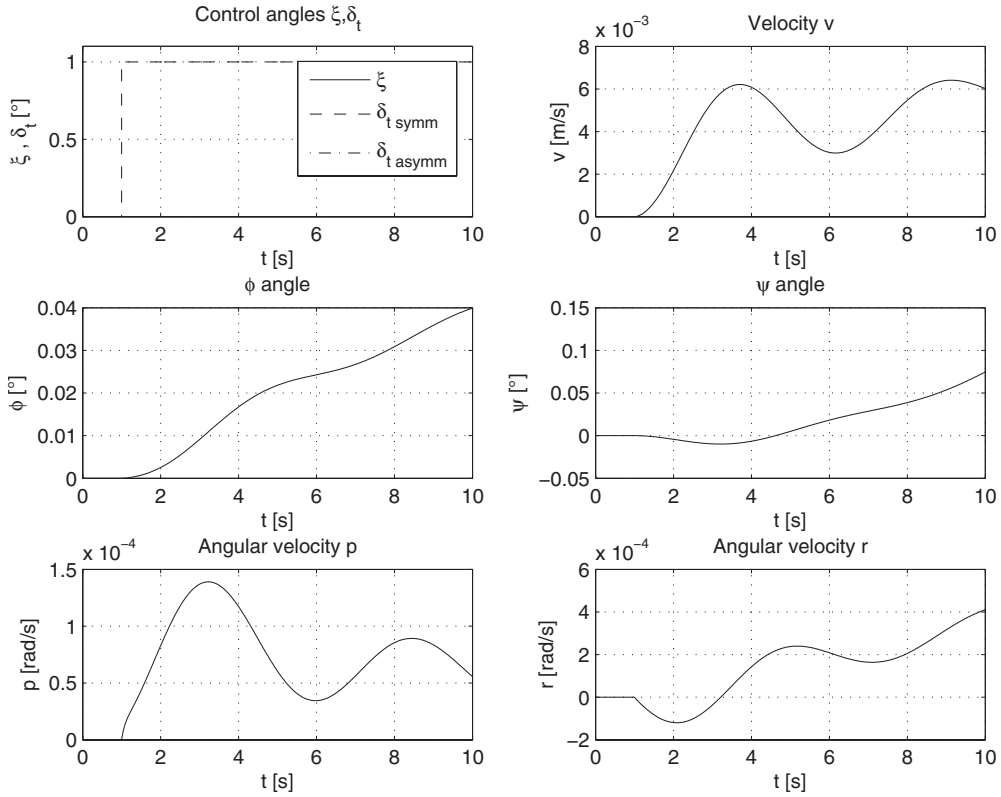

Fig. 19. Lateral response to a step $\delta_{t\ \mathrm{symm}}=1°$, deflection in the same way

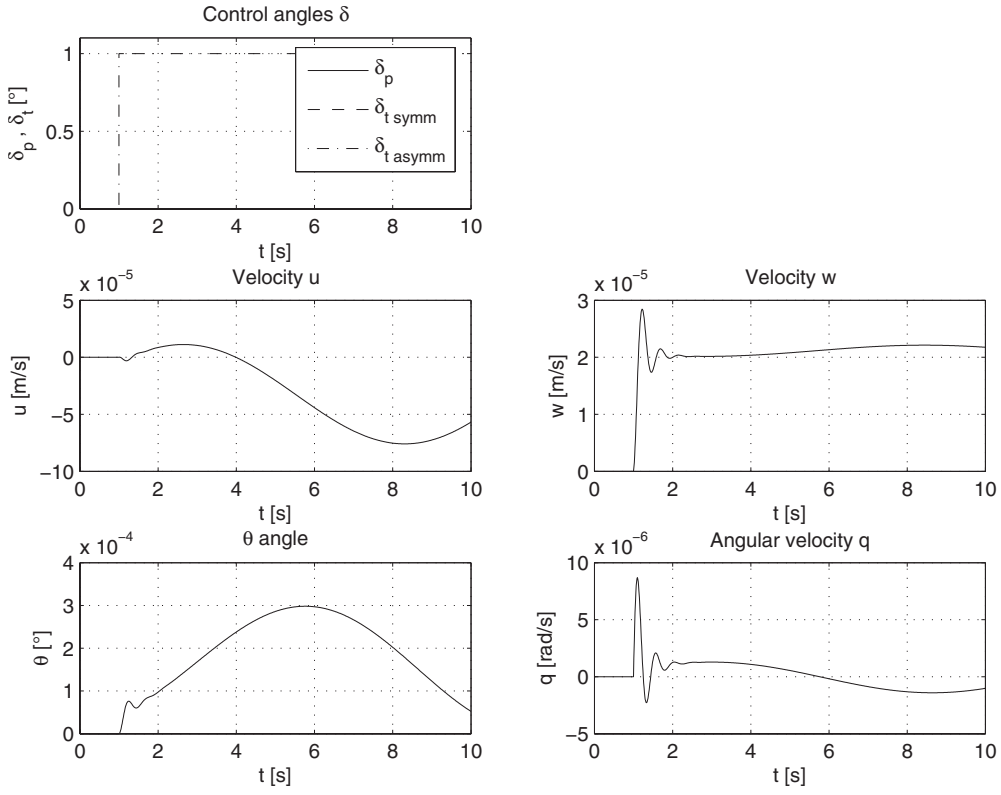

Fig. 20. Longitudinal response to a step rudder deflection, opposite direction

J. Aerosp. Eng. 2010.23:251-264.

start to climb. The pilot cannot reduce further the incidence and lift becomes larger than the airplane weight. It is noticed that the thrust coefficient decreases while the velocity is increasing. The dimensionless coefficient of thrust is divided by the square of the velocity.

Dynamic Stability

To analyze the trike's dynamic stability the eigenvalues of the linear systems, Eq. (17) and Eq. (18), are computed. In Figs. 13 and 14 the root loci of longitudinal and lateral motion are reported, respectively. These diagrams are obtained for different values of the flight speed.

Looking at the longitudinal results, it is easy to see a classical short period motion and the phugoid roots. The two eigenvalues relates short period are largely stable and the stability is improved by a speed increasing. The frequency of this motion is very high and it increases by increasing the speed. The phugoid mode is stable for high velocities and becomes unstable by reducing the speed. The motion has a very low damping/amplification and frequency. Also for this motion an increase of the flight speed causes an increase of the damping as well as a reduction of the frequency.

By looking at the lateral eigenvalues, the three classical modes were found (1) roll subsidence; (2) spiral mode; and (3) dutch roll. Thanks to the pendulum effect the roll subsidence is largely stable, the dutch roll is stable but it could become bothersome. The spiral mode is unstable but the *time to double* it is high enough.

Effects on Stability: Modified Wing Configuration

Analyzing the effects of the fins on the trikes dynamic stability, only the lateral modes are affected, see Figs. 15 and 16. Looking at Fig. 15, it is noticeable that the effects of fins on longitudinal modes are negligible. This happens because the fins are too small compared to wing and their inclination is too small to generate significant vertical forces and moments in the longitudinal plane.

Considering now the lateral-directional modes, the roll subsidence mode seemed to be not influenced by the vertical surfaces. This happens as said above, because the surfaces are small and the arm length is too small to generate large moments around the x-axis.

The improvements in lateral dynamics caused by fins are easy to find in both Dutch roll and spiral modes. In spiral mode fins cause an increase of the time to double and for high speeds the motion becomes stable. At the speed that spiral mode becomes stable, a $-\infty,+\infty$ discontinuity in the graph is noted. Negative values indicate a time to double and positive ones a time to half. Considering the Dutch roll mode, the fins cause an increment in the frequency of oscillations, the real part of the eigenvalues results in more negatives for almost all speeds, so the *time to half* is shorter.

Response to Control Inputs

In this section, time response of the trike has been analyzed for several controls. Only the results obtained with a unitary step control are reported, for multiple steps or ramp controls see Carrera and Cosatto (2008). As control, both undercarriage position and deflection of mobile surfaces has been considered.

Considering the classical technique of piloting, in Fig. 17 the response to a unitary step in longitudinal control variable δ is reported, and in Fig. 18 the response to a variation of ξ. In longitudinal response it is easy to find the effects of the short period, high frequency well damped oscillations just after the step. The low frequency phugoid mode, which is at that speed unstable, is noticeable too. In the lateral response the oscillations are caused by the Dutch roll and are damped.

In Fig. 19 the response to a unitary deflection of mobile surfaces in the same way, $\delta_{t\ \mathrm{symm}}$, is shown. This kind of deflection influences only lateral variables, so the longitudinal response is not reported. Looking at the diagrams, the effects of Dutch roll as damped oscillations are clearly visible. Just after the step an adverse yaw is present. By comparing these results with those obtained using the weight shifting technique, deflecting the rudders gives a response of two magnitude orders less than the other method. Deflecting the mobile surfaces in opposite directions, $\delta_{t\ \mathrm{asymm}}$, only effects in the longitudinal motion are seen, see Fig. 20. Lateral forces will delete each other and the moment will be null. Because of the small lateral inclination of the fins, their small surface and the small arm length, the response to this control is about four magnitude orders less than the weight shifting technique. This deflection of the rudders could be anyway useful to trim the trike with a smaller control angle δ_p.

Conclusions

In this work, a mathematical model to study the dynamic behavior of a trike ultralight aircraft is developed. To do that, in order to take into account the engine thrust. The necessary changes have been made on models developed for hang gliders.

A numerical assessment with the hang glider reference results is made and a good agreement with trimmed quantities is found. The stability results are quite different because there are no sufficient information about the wing to obtain the same wing aerodynamic derivatives as in De Matteis (1991) is given.

Then the rigid wing trike flight dynamics has been analyzed. The effect of the thrust does not causes big variations on the behavior of the plane. A bigger separation between short period and phugoid with respect to the hang glider is noted. It is caused by both the increased mass of the undercarriage and the increased flight speed. Now it is also important to consider the engine's mass, the fuel and the second pilot. The phugoid motion is seen to be stable for high flight speeds but unstable at lower ones, whereas the short period is seen as always stable and well damped.

Analyzing the lateral motion, the classical three lateral modes were found: roll subsidence, Dutch roll, and the spiral mode. The first two are stable and well damped, but the spiral mode is unstable. Fortunately the time to double is high enough to allow the pilot to correct it.

The modified wing configuration suggested by Cannone (2006) has been also analyzed. On this rigid wing, two little vertical surfaces are added. Analyzing the effects on the stability of these fins, their effect on longitudinal motion is negligible, but an improvement in lateral stability is found. In particular the spiral mode presents higher time to double and becomes stable for high speeds and also dutch roll is improved.

At the end, the time response to pilot controls has been studied. Both weight shifting controls and deflections of the rudders were studied. The two rudders can be deflected in both same and opposite direction. If the rudders were deflected in the same way only lateral motion is affected while for opposite deflections only a variation in the pitching moment is obtained. The deflection of the rudders have an effectiveness of two magnitude orders less

J. Aerosp. Eng. 2010.23:251-264.

than the weight shifting in lateral motion and about four for the longitudinal one.

Acknowledgments

This work has been carried out in the framework Piedmont Regional Project E40.

Notation

The following symbols are used in this paper:

$(.)_b$ = indicates the partial derivative of A respect to b;
C_A = dimensionless coefficient of the quantity A;
cg, cg_w, cg_p = center of gravity of the whole aircraft, the wing's center of gravity, and the pilot/undercarriage one, respectively;
$\mathbf{F}$ = force vectors in x-,y-,z-directions $\{X, Y, Z\}$;
L, D = lift and drag forces, respectively;
$\mathbf{M}$ = moment vectors around x-,y-,z-directions $\{L, M, N\}$;
$m, \mathbf{I}$ = mass and the inertia matrix of the whole aircraft;
$oxyz, oxz$ = reference orthogonal fixed body axes system and the symmetry plane;
T = thrust force generate by the propeller;
$\mathbf{v}, \dot{\mathbf{v}}$ = cg's velocity and acceleration vectors in x, y, z directions $\{u, v, w\}$, $\{\dot{u}, \dot{v}, \dot{w}\}$;
x_p, y_p, z_p = pilot /undercarriage's cg coordinates;
x_w, y_w, z_w = wing's cg coordinates;
α, β = angle of attack and sideslip angle, respectively;
$\delta, \xi, \delta_{\text{th}}$ = longitudinal, lateral control angles, and the thrust control, respectively;
$\delta_{t_{\text{symm}}}, \delta_{t_{\text{asymm}}}$ = symmetrical and the antisymmetrical use control angle of added vertical surfaces;
ϕ, θ, ψ = Euler rotation angles;
ω = angular velocity around x, y, z directions vector $\{p, q, r\}$;
$(.)_{\text{eq}}$ = indicates a steady equilibrium quantity;
$(.)_g, (.)_a$ = indicates gravitational or aerodynamic force or moment vector;
$(.)_p, (.)_w$ = indicates that the quantity is related respectively to the pilot/undercarriage or to the wing; and
$(.)^*$ = equivalent derivatives. These are obtained by collecting the terms for each variables to simplify the notation.

References

Cannone, L. L. (2006). "Analisi di Deltaplano con Ala Rigida in Materiale Composito [Analysis of trike with rigid wings made by composite materials]." Master's thesis, Politecnico di Torino, Torino, Italy.

Carrera, E., and Cosatto, C. (2008). "Analisi delle caratteristiche dinamiche di un deltaplano a motore ad ala rigida [Dynamic response analysis of a motorized trike with rigid wing]." *Rep. No. 34/2008*, DIASP, Politecnico di Torino, Torino, Italy.

Cook, M. V. (1994). "The theory of the longitudinal static stability of the hang glider." *Aeronaut. J.*, 98(978), 292–304.

De Matteis, G. (1991). "Dynamics of hang gliders." *J. Guidance*, 14(6), 1145–1152.

Drela, M., and Youngren, H. (2008). "AVL, aerodynamic analysis, trim calculation, dynamic stability analysis, aircraft configuration development, GNY general public license." *Technical documentation*, ⟨http://web.mit.edu/drela/Public/web/avl/⟩.

Etkin, B. (1995). *Dynamics of flight: Stability and control*, 3rd Ed., Wiley, New York.

Grande, F. (2007). "Progetto ed Analisi di un Deltamotore con ala in Materiale Composito [Design and analysis of trike with wings made by composite materials]." Master's thesis, Politecnico di Torino, Torino, Italy.

Kilkenny, E. A. (1984). "Full scale wind tunnel tests on hang glider pilots." *Rep. No. 8416*, College of Aeronautics, Cranfield Institute of Technology, Cranfield, U.K.

Kilkenny, E. A. (1986). "An experimental study of the longitudinal aerodynamic and static stability characteristics of hang gliders." Ph.D. thesis, College of Aeronautics, Cranfield Institute of Technology, Cranfield, U.K.

Spottiswoode, M., and Cook, M. V. (2006). "Modelling the flight dynamics of the hang glider." *Aeronaut. J.*, 110(1103), 1–20.